



UNIVERSITI PUTRA MALAYSIA

**THERMAL AND SPECTRAL RESPONSE CHARACTERISATION OF
SOLID SAMPLES USING PHOTOTHERMAL TECHNIQUE**

LING YOKE TING

FSAS 2001 21

**THERMAL AND SPECTRAL RESPONSE CHARACTERISATION OF SOLID
SAMPLES USING PHOTOTHERMAL TECHNIQUE**

By

LING YOKE TING

**Thesis Submitted in Fulfilment of the Requirement for the Degree of Master of
Science in the Faculty of Science and Environmental Studies
Universiti Putra Malaysia**

November 2001



SPECIALLY DEDICATED TO:

My beloved parents : **Ling Eng Meow**
 Lee Ee Hiong
Brothers : **Ling Choo Chuen, Ling Choo Yeun, Ling Choo Shiuh**
Sister : **Ling Yoke Mei**
Sister in law : **Foong Pui San**
Brother in law : **Tony Wong Yee Min**
Nephew : **Ling Qi Wen, Ling Qi Hua, Andrew Wong**
Niece : **Abby Wong**
Friends : **Lim Kean Pah, Fanny Chin, Teh Chze Ling, Teh Ee Phing,**
 Cheah Fun Ling, Kak Shidah.

Thank you for your wonderful encouragement and support.

Also to **Dr. Azmi Zakaria** for his guidance, advice and endless support and understanding. Words of thanks is also dedicated to Eow Wat Son for the love and care which really helped a lot in giving me moral support to complete this **Master of Science (Physics)** thesis.

Abstract of thesis presented to the Senate of Universiti Putra Malaysia in fulfilment of requirement for the degree of Master of Science

**THERMAL AND SPECTRAL RESPONSE CHARACTERISATION OF SOLID
SAMPLES USING PHOTOTHERMAL TECHNIQUE**

By

LING YOKE TING

November 2001

Chairman : Azmi Zakaria, Ph.D.

Faculty : Science and Environmental Studies

In this study, a polyvinylidene difluoride (PVDF) film was used as a pyroelectric detector in the lateral distance scanning technique to determine the thermal diffusivity of solid samples. The samples of interest were aluminium, copper and spray paint. The values obtained were $0.809\text{cm}^2\text{s}^{-1}$, $1.131\text{cm}^2\text{s}^{-1}$ and $1.547\times 10^{-3}\text{cm}^2\text{s}^{-1}$ respectively. The values were very close to the values obtained by previous works.

Next, the open photoacoustic cell (OPC) technique was used for measuring thermal diffusivity of ferrite samples. The values obtained were in the range of $0.3\text{cm}^2\text{s}^{-1}$ to $0.5\text{cm}^2\text{s}^{-1}$. EDAX analysis proved that zinc loss happened when the sample was sintered at high temperature and the loss was accompanied by sample shrinkage and density increment. Thus, the thermal diffusivity value increased with the amount of zinc loss during the sintering process.

A photopyroelectric spectroscopic (P²ES) technique was developed and applied to solid samples such as poly-methylmethacrylate doped with methylene red (PMMA-MR), poly-methylmethacrylate doped with Rhodamine B (PMMA-RB) and plant leaves to see the absorption and transmission spectrum range of samples. The spectra obtained showed that they were of transmission type as predicted by Mandelis and Zver. The sample condition, that was $\mu_s < L_s$, $l_\beta > L_s$, in obtaining the spectrum agreed with Mandelis and Zver's predictionⁱⁱ. The trend of optical transmission spectrum for doped PMMA-MR suggests that it could be used as a cut off filter in the range of 525nm and below to 400nm. The spectrum of PMMA-RB showed an absorption range between 500 to 550nm and a highly transmitted region above 600nm. The P²E spectra of leaf obtained were in line to the leaf absorption spectrum obtained by Lima et al. A young leaf has a higher signal compared to a mature leaf because it is thinner and thus the optical absorption length is longer than the mature leaf. At the saturated transmission spectral region, the logarithmic signal of all these samples was found decreasing linearly with square root of chopping frequency, agreeing to Rosencwaig and Gersho's prediction. The spectrum of ferrite samples showed that the spectrum was similar to that of light source because its optical length, l_β , was still small compared to sample thickness, L_s .

Abstrak tesis ini dikemukakan kepada Senat Universiti Putra Malaysia sebagai memenuhi keperluan untuk ijazah Master Sains

PENGELASAN CIRI-CIRI TERMA DAN SIGNAL SPECTRUM BAGI SAMPEL PEPEJAL DENGAN MENGGUNAKAN TEKNIK FOTOTERMA

Oleh

LING YOKE TING

November 2001

Pengerusi : Azmi Zakaria, Ph.D.

Fakulti : Sains dan Pengajian Alam Sekitar

Dalam kajian ini, pengesanan fotopiroelektrik (PVDF) telah digunakan pada teknik penganjakan jarak sisi untuk menentukan nilai kerosapan terma bagi sampel pepejal seperti aluminium, kuprum dan cat hitam. Nilai kerosapan terma yang diperolehi untuk sampel-sampel tersebut adalah masing-masing $0.809\text{cm}^2\text{s}^{-1}$, $1.131\text{cm}^2\text{s}^{-1}$ dan $1.547 \times 10^{-3}\text{cm}^2\text{s}^{-1}$. Nilai-nilai yang diperolehi ini didapati amat hampir berbanding nilai-nilai literatur.

Teknik fotoakustik sel terbuka (OPC) juga digunakan untuk menentukan nilai kerosapan terma bagi sampel ferit. Nilai yang diperolehi adalah di dalam julat $0.3\text{cm}^2\text{s}^{-1}$ hingga $0.5\text{cm}^2\text{s}^{-1}$. Analisa EDAX membuktikan bahawa kehilangan zink berlaku ketika sampel di sinter pada suhu tinggi. Proses kehilangan ini diiringi dengan pengecutan sampel dan peningkatan ketumpatan sampel. Jadi, nilai kerosapan terma ferit meningkat dengan peningkatan kehilangan zink semasa proses pensinteran.

Suatu teknik spektroskopi fotopiroelektrik (P^2ES) telah dibina dan digunakan untuk mengkaji sampel pepejal seperti polimetilmetakrilat yang didopkan dengan metil merah (PMMA-MR) dan Rhodamine B (PMMA-RB) serta sampel daun untuk melihat spektrum penyerapan dan transmisi sampel-sampel tersebut. Spektra yang diperolehi adalah jenis spektrum transmisi seperti yang dianggarkan oleh Mandelis dan Zver. Syarat-syarat yang dicapai ketika itu ialah $\mu_s < L_s$, $l_\beta > L_s$ dan keadaan ini adalah seperti yang dijangkakan oleh Mandelis dan Zver. Bentuk spektrum PMMA-MR yang diapati mencadangkan bahawa sampel ini boleh digunakan sebagai penuras cahaya pada julat panjang gelombang kurang daripada 525nm hingga ke 400nm. Spektrum PMMA-RB menunjukkan penyerapan pada julat panjang gelombang 500nm sehingga 550nm dan amat bertransmisi pada julat 600nm ke atas. Spektra P^2E bagi sampel daun menunjukkan persetujuan dengan spektra penyerapannya seperti yang diperolehi oleh Lima et al. Signal spektra bagi daun muda menunjukkan nilai yang lebih tinggi berbanding dengan daun matang kerana keratan rentasnya yang lebih nipis dan ini menyebabkan jarak optiknya yang lebih panjang berbanding dengan daun matang. Pada keadaan spektra transmisi tepu, signal logaritma bagi semua sampel di atas berkurang secara linear apabila diplotkan berlawanan dengan punca kuasa dua frekuensi pencantas optik dan ini adalah benar berdasarkan anggaran Rosencwaig dan Gersho. Spektrum sampel ferit menyerupai spektrum lampu rujukan kerana jarak penyerapan optiknya, l_β , adalah lebih kecil daripada tebal sampel, L_s .

ACKNOWLEDGEMENTS

First of all, I would like to express my deepest praise to God who has allowed and given me all the strength, faith, confidence and patience to complete this project within the time frame despite all the challenges.

It would be my pleasure to express my most sincere gratitude and highest thanks to my project supervisor Dr. Azmi Zakaria for his invaluable guidance, assistance, help, patience and advice throughout those years. I would also like to extend my appreciation to my co-supervisors, Associate Professor Dr. Wan Mahmood Mat Yunus and Associate Professor Dr. Mansor Hashim for advice and helpful discussion during this period of time.

Special thanks is also given to Pn. Astuty and En. Nasri from Material Engineering laboratory, Engineering Faculty, Universiti Teknologi Malaysia for their help on the EDAX analysis. I would also like to thank Mr. Ho and Miss. Suleka for helping me in handling the Scanning Electron Microscope (SEM) unit. I am grateful for the PASCA scholarship awarded by Universiti Putra Malaysia, which enabled me to undertake this work.

I also appreciate Pn. Norhana Yahya for her kindness and willingness to help me in sample preparation and to use the monochromator from the materials laboratory. Special thanks is credited to all the staff in Physics department especially En. Roslim for his help and co-operation given to me throughout my work. Last but not least, my sincere thanks to all friends, seniors and family members, who directly or indirectly, have contributed towards the success of the work.

This thesis submitted to the Senate of Universiti Putra Malaysia has been accepted as fulfilment of the requirement for the degree of Master of Science.

AINI IDERIS, Ph.D.
Professor
Dean of Graduate School

Date:

TABLE OF CONTENTS	PAGE
SPECIAL DEDICATION.....	ii
ABSTRACT.....	iii
ABSTRAK.....	v
ACKNOWLEDGEMENTS.....	vii
APPROVAL SHEETS.....	viii
DECLARATION FORM.....	x
LIST OF TABLES.....	xiii
LIST OF FIGURES.....	xiv
LIST OF ABBREVIATIONS.....	xviii
LIST OF SYMBOLS.....	xix

CHAPTER

1. INTRODUCTION

1.1. Photothermal Processes.....	1
1.2. Spectroscopy in General.....	4
1.3. Photopyroelectric Detection.....	5
1.4. Advanced Material.....	8
1.5. Objectives.....	9

2. LITERATURE REVIEW

2.1. Photothermal Spectrometer.....	10
2.2. Literature Review on Open Photoacoustic Cell Technique.....	13
2.3. Literature Review on Photopyroelectric Spectrometer.....	15
2.4. Introduction on Ferrites.....	19
2.5. Literature Review of Ferrites.....	21
2.6. Literature Review on Polymer Films Poly-(Methyl) Methacrylate:.....	25

3. THEORY

3.1. Theory of Photopyroelectric Effect.....	28
3.1.1. Special Cases.....	35
3.1.2. Quality of A Spectrum.....	43
3.1.3. Absorption Spectroscopy.....	45
3.1.4. Absorption Spectroscopy of Biological Samples.....	50
3.2. Theory on Ferrites.....	57
3.2.1. Spinel Ferrites.....	58
3.2.2. Microstructure.....	60

4. METHODOLOGY

4.1. Developing of Photopyroelectric Spectrometer System.....	63
4.1.1. Stepper Driver and Stepper Motor.....	64
4.1.2. Power Supply.....	68
4.1.3. Photodiode.....	69
4.1.4. Water Filter.....	70

4.1.5. Lock-in Amplifier (SR 530).....	71
4.1.6. Light Source.....	72
4.1.7. Noise.....	73
4.1.8. Normalisation of PVDF Spectrum.....	75
4.2. Photopyroelectric Measurement of The Thermal Diffusivity of Solids.....	76
4.3. Preparing Ferrite Samples.....	78
4.4. Open Photoacoustic Cell.....	84
4.5. Preparing Poly(methyl)-methacrylate Sample.....	86
4.6. Calibration of The Photopyroelectric Spectrometer.....	87
5. RESULTS AND DISCUSSION	
5.1. Thermal Diffusivity Measurement of Aluminium, Copper and Spray Paint by Lateral Distance Scanning Photopyroelectric Method.....	97
5.2. Thermal Diffusivity for Ferrite by Open Photoacoustic Cell...	101
5.3. Photopyroelectric Spectroscopy of Doped PMMA.....	109
5.4. Spectroscopy of Leaves.....	125
6. CONCLUSION	
6.1. Conclusions.....	135
6.2. Suggestions for Future Work.....	138
BIBLIOGRAPHY.....	139
APPENDICES.....	
A.....	149
B.....	151
C.....	156
D.....	161
E.....	173
F.....	175
PUBLISHED WORK.....	183
VITA.....	185

LIST OF TABLES

Table		Page
2.1	Applications of Produced NiZn Ferrites.....	20
3.1	Properties of photosynthetic pigments.....	51
3.2	The Advantages of Soft Ferrites.....	58
5.1	The Comparison of Present Value to The Literature Values.....	99
5.2	The Comparison of Present Value to The Literature Values.....	100
5.3	Comparison of Thermal Diffusivity Value for Spray Paint with Literature Data.....	100
5.4	The Thermal Diffusivity Values of Sample Ferrite of Different Zinc Oxide Composition.....	105
5.5	The Percentage of Zn left in Final Product of 5 Ferrite Samples, Obtained from EDAX Analysis.....	106

LIST OF FIGURES

Figures		Page
1.1	The processes involved in photothermal spectroscopy.....	4
3.1	One dimensional geometry of a photopyroelectric system.....	30
3.2	A composite trilayered sample.....	45
3.3	Normalised photothermal (a) absorption spectrum and (b) transmission spectrum of 0.8×10^{15} Nd_2O_3 molecules in a $1\mu\text{m}$ thick PMMA film coated on top of 0.1mm undoped PMMA spread on a silver substrate. recorded by out-of-phase detection at (a) 2.2Hz and (b) 88Hz modulation frequency.....	46
3.4	Schematic diagram and graph of the light absorption in thick Sample. Here the signal is proportional to $(1-L_s\beta_s)$	47
3.5	Absorption spectrum of aqueous solutions of Rhodamine B at 22°C , O $1.5 \times 10^{-3}\text{M}$, X $7.6 \times 10^{-4}\text{M}$, \square $3.0 \times 10^{-6}\text{M}$	48
3.6	The molecule structure of Rhodamine B.....	49
3.7	The cross section of a leaf showing the inhomogeneous sample leaf with multilayers of cells.....	50
3.8	Solid line shows the absorption spectrum of chlorophyll a in ether (Holt and Jacobs, 1954) while dashed line shows the red absorption band of chlorophyll a in microcrystalline state, note the shift of 80nm towards longer wavelength and dotted lines shows the fluorescence emission spectrum of the ether solution.....	53
3.9	Absorption spectrum of a whole spinach leaf, cooled to -196°C . Note maxima due to chlorophyll b at 650nm, two major binding states of chlorophyll a (~ 670 and 680nm respectively) and a minor, long wave chlorophyll a fraction ($\sim 705\text{nm}$).....	53
3.10	Spinel's structure.....	59
4.1	(a) One dimensional geometry of a pyroelectric-sample assembly. (b) The schematic diagram of the spectrometer.....	63
4.2	The lens used to focus the light into the monochromator input slit.....	64
4.3	The phototransistor 308-613 and its connections.....	67
4.4	The unipolar stepper driver board diagram.....	68
4.5	The monochromator, the stepper driver, stepper motor and the power supply used in this work.....	68
4.6	Power supply circuit diagram.....	69
4.7	Circuit for photodiode photo-detector.....	70
4.8	The side view of a water filter.....	71
4.9	The front panel view of the lock-in amplifier (SR530).....	72
4.10	The one-kilowatt Xenon arc lamp (light source) and its power supply (Oriol 6269).....	73
4.11	Noise spectrum.....	74
4.12	The mechanical chopper and pre-amplifier.....	75

4.13	(a) Schematic diagram of the experimental setup used for measuring thermal diffusivity, (b) Schematic configuration of the sample-PVDF film lateral-heating method for measuring thermal diffusivity.....	78
4.14	Flow chart for sample preparation.....	81
4.15	The schematic cross section of open photoacoustic cell detector.....	84
4.16	The graph shows the linear increases of P ² E signal with the light power at various chopping frequencies.....	88
4.17	Graph shows the increase of P ² E signal with the increase of sample illuminative area.....	89
4.18	The resolution of carbon spectrum improved as monochromator slit width decreases.....	89
4.19	The graph shows the signal of the reference photodiode positioned at the side of apparatus.....	90
4.20	The spectrum of raw carbon using PVDF detector.....	91
4.21	Spectrum of normalized carbon signal using PVDF detector.....	91
4.22	Plot of He-Ne laser spectrum of various light intensity at 10micron monochromator slitwidth and at 2×10^4 amplifier gain.....	92
4.23	Plot of height peak spectrum at various light intensity at 10micron monochromator slitwidth.....	93
4.24	Spectrum of Helium-Neon laser linewidth at various monochromator slitwidth.....	94
4.25	Linear dependence of the spectral linewidth against the monochromator slitwidth.....	94
4.26	Linear dependence of the spectrum's peak height against the monochromator slitwidth.....	95
4.27	The spectrum of normalized signal of ferrite sample.....	95
5.1	The graph of ln signal versus lateral distance for aluminium.....	98
5.2	The graph of ln signal versus lateral distance for copper.....	98
5.3	The graph of ln signal versus lateral distance for spray paint.....	99
5.4	The graph shows the kink of open cell's photoacoustic signal for ferrite $\text{Ni}_{1-x}\text{Zn}_x\text{Fe}_2\text{O}_4$ when $x=0.1$ and sintered at 1250°C.....	103
5.5	The graph shows the kink of open cell's photoacoustic signal for ferrite $\text{Ni}_{1-x}\text{Zn}_x\text{Fe}_2\text{O}_4$ when $x=0.1$ and sintered at 1300°C.....	103
5.6	The graph shows the kink of open cell's photoacoustic signal for ferrite $\text{Ni}_{1-x}\text{Zn}_x\text{Fe}_2\text{O}_4$ when $x=0.1$ and sintered at 1350°C.....	104
5.7	The trend in changes of thermal diffusivity value with the different Zinc oxide composition.....	108
5.8	The graph shows the loss of Zinc increases with the increase of sintering temperature for each x value of Zn composition in the NiZn ferrite prepared.....	108
5.9	The graph shows the thermal diffusivity value for ferrite sample increases linearly with its density value.....	109
5.10	Comparison of the P ² E spectrum for 1.6×10^{-3} mmole g ⁻¹ concentration of Methylene red respectively at chopping frequency 60, 70, 80 and 90Hz to the optical transmission spectrum of conventional	

	spectrophotometer (-□).....	112
5.11	Comparison of the P ² E spectrum for 3.1x10 ⁻³ mmole g ⁻¹ concentration of Methylene red respectively at chopping frequency 60, 70, 80 and 90Hz to the optical transmission spectrum of conventional spectrophotometer (-□-).....	112
5.12	Comparison of the P ² E spectrum for 4.7x10 ⁻³ mmole g ⁻¹ concentration of Methylene red respectively at chopping frequency 60, 70, 80 and 90Hz to the optical transmission spectrum of conventional spectrophotometer (-□-).....	113
5.13	Comparison of the P ² E spectrum for 6.3x10 ⁻³ mmole g ⁻¹ concentration of Methylene red respectively at chopping frequency 60, 70, 80 and 90Hz to the optical transmission spectrum of conventional spectrophotometer (-□-).....	113
5.14	The graph for PMMA-MR for different concentrations of Methylene red at various chopping frequency and at 650nm.....	114
5.15	The graph for PMMA-MR for different concentrations of Methylene red at various chopping frequency and at 475nm.....	115
5.16	The figure shows the spectrum for PMMA-MR at 60Hz chopping frequency and at 3.1x10 ⁻³ mmole g ⁻¹ , 4.7x10 ⁻³ mmole g ⁻¹ , 6.3x10 ⁻³ mmole g ⁻¹ concentration of MR.....	116
5.17	The spectrum shows the comparison of PMMA-RB doped with 1.044x10 ⁻⁴ mole l ⁻¹ (r1) and 4.175x10 ⁻⁴ mole l ⁻¹ (r2) Rhodamine B at 60Hz chopping frequency.....	118
5.18	The spectrum shows the PMMA-RB spectrum normalized with photodiode signal rather than using carbon.....	118
5.19	The spectrum shows the comparison of PMMA-RB doped with 1.044x10 ⁻⁴ mole l ⁻¹ (r1) Rhodamine B at 60, 70, 80, and 90Hz chopping frequency	119
5.20	The spectrum shows the comparison of PMMA-RB doped with 4.175x10 ⁻⁴ mole l ⁻¹ (r2) Rhodamine B at 60, 70, 80 and 90Hz chopping frequency.....	119
5.21	The graph signal at various chopping frequency of PMMR-RB sample r1 and r2 at 525nm.....	120
5.22	The graph shows at various chopping frequency of PMMR-RB sample r1 and r2 at 650nm.....	120
5.23	The optical transmission spectra of PMMA-RB with 3.76x10 ⁻³ mole l ⁻¹ concentration of Rhodamine B.....	122
5.24	The voltage signal versus time of the sample PMMA-RB by using flash technique.....	124
5.25	The voltage signal versus time of the sample PMMA-RB by using flash technique.....	124
5.26	The voltage signal versus time of the sample PMMA-RB by using flash technique.....	125
5.27	The spectra of matured green leaf <i>Ficus benjamina</i> L. from Moraceae family with the thickness of 0.232mm at 60, 70, 80 and 90Hz chopping frequency.....	127

5.28	The spectra of young green leaf <i>Ficus benjamina</i> L. from Moraceae family with the thickness of 0.147mm at 60, 70, 80 and 90Hz chopping frequency.....	127
5.29	The graph of logarithmic signal versus square root of chopping frequency of young leaf of thickness of 0.147mm and leaf of thickness of 0.232mm, both at 550nm wavelength.....	128
5.30	The spectra of <i>Imperata cylindrical</i> (green leaf) from Graminae family transmission spectra at 60 and 70 80Hz chopping frequency.....	129
5.31	The spectra shows the comparison of <i>Cyanthula sp.</i> (red leaf) from Amaranthaceae family with the thickness of 0.110mm at 60, 70, 80 and 90Hz chopping frequency.....	129
5.32	The graph shows the decrease of logarithmic signal with square root of frequency at three different wavelength of red leaf sample.....	130
5.33	The spectra of yellow leaf <i>Codiaeum variegatum</i> L. ver. <i>Pictum</i> (Lod.) Muell. Arg. from Euphorbiaceae family with the thickness of 0.207mm and at 60, 70, 80 and 90Hz chopping frequency.....	131
5.34	The graph of signal versus square root of chopping frequency at 650nm wavelength.....	132
5.35	The spectra of yellow paper at 60, 70, 80 and 90Hz chopping frequency.....	133
5.36	The spectra of the green paper at 10, 60, 70 and 80Hz chopping frequency.....	133

LIST OF ABBREVIATIONS.

PVDF	Polyvinylidene fluoride
P ² E	Photopyroelectric
P ² ES	Photopyroelectric Spectroscopy
PAS	Photoacoustic Spectroscopy
PMMA-MR	Poly (methyl)-methacrylate doped methylene red
PMMA-RB	Poly (methyl)-methacrylate doped Rhodamine B
He-Ne	Helium-Neon laser
EDAX	Energy Dispersive X-ray Analysis
SEM	Scanning electron microscopy
QBASIC	Quick basic programming
OPC	Open photoacoustic detection

LIST OF SYMBOLS

μ_s	= Thermal diffusion length	L_b	= Backing's thickness
L_s, l_s	= Sample's thickness	C	= Capacitance
l_β	= Optical absorption length	K	= Dielectric constant
α_s	= Thermal diffusivity value	L_p	= Pyroelectric's thickness
π	= Pi	η	= Nonradiative conversion efficiencies
f	= Frequency	θ	= Temperature
f_c	= Characteristic frequency	x	= Distance
Fe^{2+}	= Divalent ferrous ions	ϵ_0	= Vacuum permittivity
Fe^{3+}	= Trivalent ferric ions	μ_β	= Optical absorption length
e	= Electron	b	= Backing
Zn^{2+}	= Zinc ion	k	= Thermal conductivity
Ni^{2+}	= Nickel ion	ρ	= Density
n	= Refractive index	C	= Specific heat capacity
V	= Voltage	μ	= Micron
ω_0	= Modulated angular frequency	O_2	= Oxygen
β	= Optical absorption length	a_s	= Thermal diffusion coefficient
λ	= Wavelength	t_d	= Sample's thickness
p	= Pyroelectric coefficient	$R(\lambda)$	= Spectral radiancy
I	= Intensity	S_c	= Spectrum's signal
t	= Time	Mg^{2+}	= Magnesium ion
ΔT	= Changes in temperature	Co^{2+}	= Cobalt ion
Q	= Charge	Li^{2+}	= Litium ion

CHAPTER 1

INTRODUCTION

1.1 Photothermal Processes

Photothermal studies cover a wide range of techniques and phenomena regarding the conversion of absorbed optical energy into heat. In the process, the optical energy is absorbed and then converted into thermal energy in a vast number of materials in solid, liquid or gas forms. It is known that the absorption of optical energy by the material is a selective process depending on the type of material used. The general heating of the material later on is caused by a series of non-radiative transitions. This happens when the excited electronic states in atoms or molecules tend to lose their gained excitation energy in the earlier process.

In the mid 1970s, an alternative of absorption spectroscopy was developed which exploited the photothermal effect. This process is called photoacoustic spectroscopy because the photothermal effect was detected by an indirect acoustic method. Photoacoustic effect has become a very important tool to investigate spectroscopic properties of any type of solid or semisolid material, in any kind of state (Manfredotti et al., 1996). In fact, as Rosencwaig (1975; 1976; 1980) has demonstrated, only the absorbed light produces an acoustic signal, while scattered light, which often presents a serious problem in conventional spectroscopy, can be neglected in photoacoustic spectroscopy (PAS), at least in a first approximation (Helander et al., 1983). In addition to the photoacoustic detection method, there are

numerous other methods which have been devised to detect photothermally generated periodic heating. These include the piezoelectric effect, the pyroelectric effect, the emission of infrared radiation, the mirage effect, the modulation of the surface optical reflectance and the detection of the thermally induced surface distortion.

The photothermal technique is well known because it is a nondestructive technique (NDT) where the sample is not destroyed and still can be further investigated. This photothermal technique has the flexibility in signal detection to suit particular requirements.

In the photothermal effect, thermal waves are produced by the periodic heating of the surface of the sample by a modulated light source and interact with thermal inhomogeneities as they travel within the sample material. This thermal waves will experience a few processes such as scattering, reflection, refraction and diffraction. The signal detected due to these processes occurring at subsurface boundaries, will depend on the relative position of the heat source and the detector used. The amount of energy absorbed varies as it depends on the surface properties.

Thermal wave detection techniques were classified into three groups, which are acoustic, optical and thermal methods. The acoustic detection technique uses either a gas condenser microphone for pressure variations detection or a piezoelectric transducer for thermoelastic waves detection in solid media. On the other hand, the thermal detection technique includes the use of thermistors, thermocouples, infrared detectors, photothermal radiometry (PTR) or pyroelectric transducer, which is known

as photopyroelectric detection to detect thermal waves directly. Optical methods for thermal sensing include the use of probe beams and photodetectors to monitor variations in the optical properties of a heated sample or the fluid medium adjacent to the sample. It can also be used to monitor the modulated thermal expansions of heated media by probe beam displacement techniques or via interferometry.

Photothermal spectroscopy is a study of the photo-induced change in the thermal state of samples used. It is also known as a highly sensitive method used to measure optical absorption and thermal characteristic of a particular sample. Measurements of the temperature, pressure, or density changes that occur due to optical absorption are the basis for this method.

Photothermal methods have been used to measure temperature, thermal diffusivities, sound velocity, bulk flow velocities, surface thickness and specific heats. In a homogeneous sample, the full photothermal transient is typically analyzed in order to obtain this information. However, some of these parameters can be determined by measuring signal magnitude, signal decay times, and signal onset times for carefully designed experiments. Thermal properties of heterogeneous samples can be obtained by raster scanning the optical excitation source over the sample surface. The figure 1.1 below shows the processes involved in photothermal processes.

Compared with more conventional thermal analysis methods, photothermal analysis has the advantage of noncontact generation of a well-defined heat source at the surface or in the volume of the sample of interest.

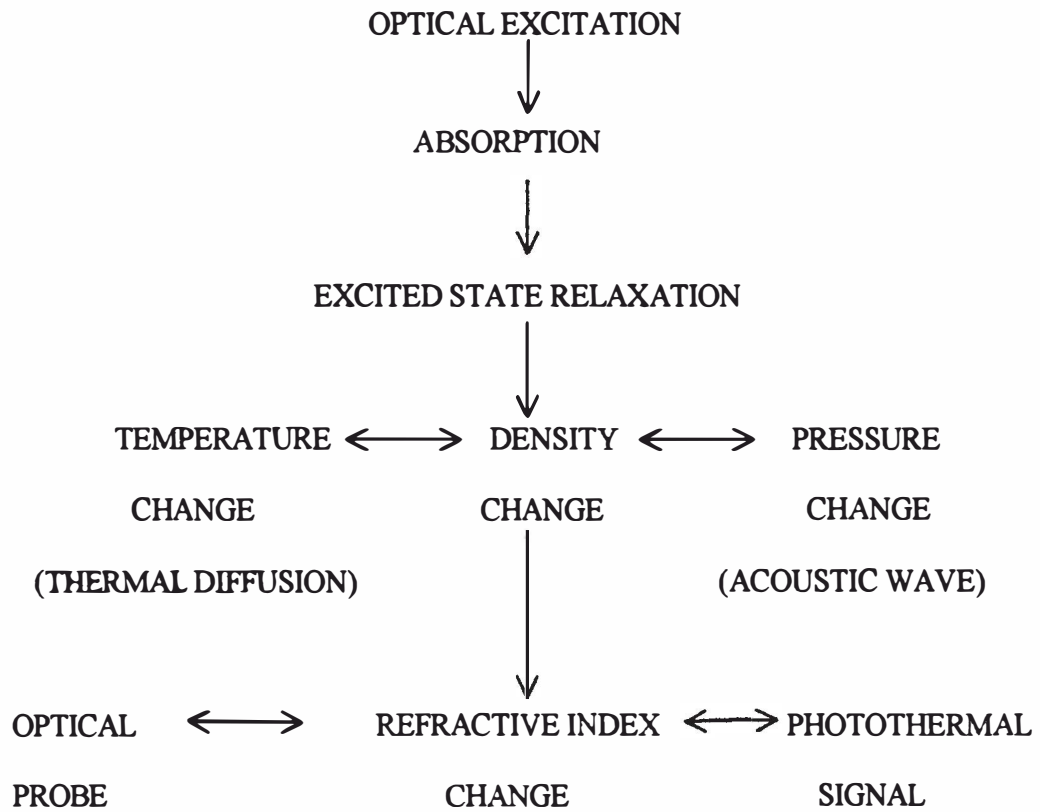


Figure 1.1: The processes involved in photothermal spectroscopy.

1.2 Spectroscopy in General

Spectroscopy is considered to have started in the year 1666 by Newton's discovery of the solar spectrum. In the year 1802, Wollaston repeated Newton's experiment and he reported that the sun's spectrum was intersected by a number of dark lines. Fraunhofer investigated these lines 21 years later and he was able to measure their wavelengths (Fraunhofer lines).

Spectroscopy is an analytic technique concerned with the measurement of the absorption or the emission interaction between the radiant energy with matter. A display of such data is called a spectrum. A spectrum is a plot of the intensity of

emitted or transmitted radiant energy versus the energy of that light. Spectra due to the absorption of radiant energy are produced when radiant energy from a stable source, collimated and separated into its components in a monochromator, passes through the sample whose absorption spectrum is to be measured and detected (Thorne, 1974).

In this study, photopyroelectric spectroscopic technique (P^2ES) was chosen as the method to characterize solid samples. In the method, a pyroelectric film detector in contact with the sample directly measures the ac temperature field generated by periodic heating. In pyroelectric material, a change in temperature gives rise to a change in its electrical dipole moment. When a charge is released to the surface of the material it creates a voltage difference that can be sensed before it is neutralised by electrical conduction, making it as an ac temperature detector. Pyroelectricity is a polar effect and only exists in materials whose structure is nonsymmetric with a unique polar axis. In this technique, the detector should be in good contact with the back of the sample. This enables the average ac temperature field produced by the transmitted thermal wave through the sample to be detected by producing a voltage across the electrodes. The electrodes are deposited on either side of the pyroelectric material. The most commonly used pyroelectric are polymer films such as polyvinylidene fluoride (PVDF or PVF_2), which is well known for its low cost.

1.3 Photopyroelectric Detection

For a pyroelectric detection to be competitive with other photothermal detection schemes a number of criteria should be met. The heat capacity of the detector should be low which means that it should have a small mass and made out